Article

Sea Lice Are Sensitive to Low Frequency Sounds

Marta Solé [1,*], Marc Lenoir [2], José-Manuel Fortuño [3], Steffen De Vreese [1], Mike van der Schaar [1] and Michel André [1,*]

1   Laboratory of Applied Bioacoustics, Technical University of Catalonia-Barcelona Tech, 08800 Vilanova i la Geltrú, Spain; steffen.de.vreese@upc.edu (S.D.V.); mike.vanderschaar@upc.edu (M.v.d.S.)
2   Institute of Neurosciences of Montpellier, INSERM, 34091 Montpellier, France; m.lenoir118@laposte.net
3   Institute of Marine Sciences, Spanish National Research Council, 08003 Barcelona, Spain; jmanuel@icm.csic.es
*   Correspondence: marta.sole@upc.edu (M.S.); michel.andre@upc.edu (M.A.)

Abstract: The salmon louse *Lepeophtheirus salmonis* is a major disease problem in salmonids farming and there are indications that it also plays a role in the decline of wild salmon stocks. This study shows the first ultrastructural images of pathological changes in the sensory setae of the first antenna and in inner tissues in different stages of *L. salmonis* development after sound exposure in laboratory and sea conditions. Given the current ineffectiveness of traditional methods to eradicate this plague, and the strong impact on the environment these treatments often provoke, the described response to sounds and the associated injuries in the lice sensory organs could represent an interesting basis for developing a bioacoustics method to prevent lice infection and to treat affected salmons.

Keywords: sea lice; *Lepeophtheirus salmonis*; acoustic trauma; transmission electron microscopy; scanning electron microscopy

1. Introduction

Ectoparasitic sea lice represent the most important parasite problem to date for the salmon farming industry. The salmon louse *Lepeophtheirus salmonis* (Figure 1) is a Caligid copepod that infests both wild and farmed salmonid fish in the northern and southern hemispheres. Salmon lice are a major disease problem in the farming of Atlantic salmon, *Salmo salar*, and it has been suggested that salmon lice also play a role in the decline of wild stocks [1,2].

Severe infestations produce pathological lesions on the host that are caused by attachment and feeding of sea lice in both the adult and juvenile stages. *L. salmonis* induces stress-related responses in the host skin and gills and modulates the immune system [3]. *L. salmonis* is exceptional among parasite species in infecting adult wild Atlantic salmon (*Salmo salar*) with 100% prevalence. The infective planktonic larva is extraordinarily effective at locating and infecting wild Atlantic salmon. For this reason, *L. salmonis* has the potential to become a pest disease to salmonid fish [2].

Understanding the nature of the interactions between *L. salmonis* and its host is crucial for identifying possible ways to resolve the negative impacts of this infection [4]. *L. salmonis* is able to detect different stimuli (e.g., pressure/moving water, chemicals and light) in its habitat. However, the response thresholds to these stimuli and the role that they play in the context of host location are still unknown. Sea lice use physical (light and salinity) and chemical (kairomones) cues to locate and recognize their host. Another fundamental sensory modality to fish location is mechanoreception through sensory organs, which allows sea lice to detect and land on their host [5].

The life cycle of *L. salmonis* includes ten stages, three of which are pelagic [1]. The third, the copepodid, represents the infective stage of the salmon louse. It carries both chemosensory aesthetes and mechanosensory setae on its antennules, indicating that both mechanical and chemical signals may be important in host-finding [6]. Initial attachment

for the copepodid normally occurs on the fish fins where it hooks into the host tissue. After some time (depending on the temperature) the copepodid undergoes a moult to the first sessile stage in the life cycle, the chalimus, which attaches itself to the fish with a penetrative thread referred to as the frontal filament [7]. Adult *L. salmonis* present different types of sensitive setae on their antennae. Heuch and Karlsen [8,9] found that salmon louse copepodids are sensitive to low frequency water accelerations such as those produced by a swimming fish.
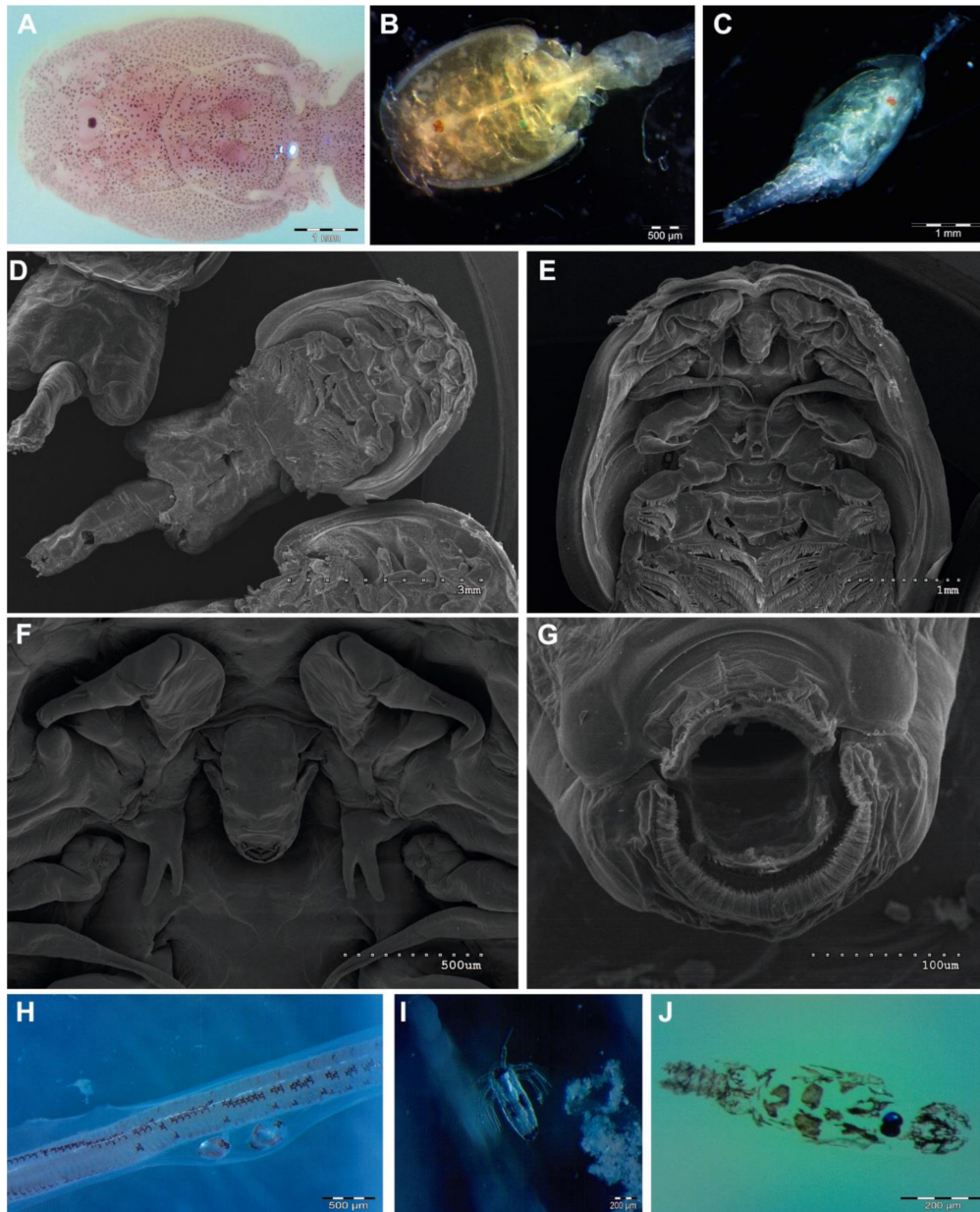

Figure 1. Light microscopy (LM) (**A**–**C**,**H**–**J**) and Scanning Electron Microscopy (SEM) (**C**–**G**). External morphology of *L. salmonis*. (**A**) Dorsal view of the head of an adult sea lice. (**B**) Dorsal view of pre-adult. (**C**) Dorsal view of chalimus. (**D**) Ventral view of the whole body of an adult *L. salmonis*. (**E**) Ventral view of a sea lice head. (**F**) Ventral view of an adult *L. salmonis* showing the mouth, maxilas and abdominal arms. (**G**) Detail of the ventral cavity showing the mouth and the three maxila. (**H**) String of sea lice eggs. In the low part of the string, two larvae are being extruded from the eggs. (**I**) Nauplius just hatched from the egg. (**J**) Copepodid of sea lice. Scale bar: (**A**,**C**,**E**) = 1 mm; (**D**) = 3 mm; (**B**,**F**,**H**) = 500 µm; (**I**,**J**) = 200 µm, G = 100 µm.

Recent findings on cephalopods [10], gastropods [11], crustaceans [12], bivalves [13] and cnidarians [14] have shown that exposure to anthropogenic noise: (i) had a direct consequence on the functionality and physiology of the statocysts, which are sensory organs responsible for these species equilibrium and movements (linear and angular accelerations) in the water column; and (ii) was challenging to the exposed individuals' survival. These experiments demonstrated the sensitivity of invertebrates to sound and described the associated pathological effects. Electron microscopy revealed injuries in the statocyst sensory epithelium after exposure to sound. The lesions present on the exposed animals were consistent with the manifestation of a massive acoustic trauma observed in other species.

In contrast to other invertebrate species that require statocysts to sense the water column in order to maintain balance, zooplankters (copepods, protists) use external mechanosensors for sensing spatial velocity gradients generated by preys or predators [15]. It is understood that the absence of gravity receptors (i.e., statocysts) in planktonic animals has to do with the specific gravity of the zooplankton body, which is the same or slightly higher than water. In *L. salmonis*, these external mechanoreceptors are located on the first antenna [16].

The present study aimed at addressing the problem of sea lice infestation on salmon by using acoustic and bioacoustics techniques and by evaluating the potential effects of these techniques on the parasite's sensory organs.

2. Methods

2.1. Laboratory Experiments

We initially looked at the physiological response of lice after exposure to sound in a controlled laboratory environment.

2.1.1. Sound Exposure

Frequency

We tested a series of discrete frequencies, ranging from 100 Hz to 1 kHz. After determining which frequencies would trigger a stronger reaction to the sound exposure, we exposed with combinations of the optimal frequencies and compared the results with the discrete frequency experiments (Tables 1 and 2).

Table 1. Number of lice per frequency.

Discrete Frequencies	Number of Copepodids	
	Control	**Exposed**
100 Hz	500	500
150 Hz	500	500
200 Hz	500	500
250 Hz	500	500
300 Hz	500	500
350 Hz	500	500
400 Hz	500	500
450 Hz	500	500
500 Hz	500	500
550 Hz	500	500
600 Hz	500	500
650 Hz	500	500
700 Hz	500	500

Table 1. *Cont.*

Discrete Frequencies	Number of Copepodids	
	Control	Exposed
750 Hz	500	500
800 Hz	500	500
850 Hz	500	500
900 Hz	500	500
950 Hz	500	500
1000 Hz	500	500

Table 2. Combinations of frequencies and corresponding number of lice exposed and used as control.

Frequencies Combination	Number of Copepodids	
	Control	Exposed
350 Hz–450 Hz	500	500
350 Hz–550 Hz	500	500
450 Hz–550 Hz	500	500
300 Hz–400 Hz	500	500
400 Hz–500 Hz	500	500

Sea Lice Specimens

Fifty (50) sets of five hundred (n = 500) copepodids from *L. salmonis* were shipped to our laboratory facilities immediately after they had moulted. In the laboratory they were held in a closed system of natural seawater (at 7–10 °C, salinity 35‰) consisting of plastic tanks with a capacity of 20L until required for the experiments. An air pump facilitated the copepodid movements in the water column.

Individuals were maintained in the tank system until exposure. Several specimens (see below) were used as controls and were kept in the same conditions as the experimental animals until they were exposed to noise.

Sound Exposure Protocol

Sequential Controlled Exposure Experiments (CEE) were conducted on copepodids (25 × 500) of *L. salmonis*. A same number of copepodids (25 × 500) was used as a control and were kept in the same conditions as the exposed ones (Table 1 andTable 2).

The sound was produced and amplified through an in-air loudspeaker while the received levels were measured by a calibrated B&K 8106 hydrophone. The sound production was tuned such that each constant tone from 100 Hz to 1000 Hz was measured at 150 dB re 1 μPa^2/Hz at a fixed point in the tank.

The copepodids were exposed to sound for 4 h. The sample collection and the fixation of the lice were performed immediately after the end of the sound exposure session. The controls remained for the same time as those exposed in the isolated exposure tank (4 h) without being exposed to playback. The sacrificing process after exposure was identical for both the controls and exposed animals.

Amplitude

In this experiment, we tested the level of lice trauma after exposing them to different combinations of exposure duration, frequencies, and levels of exposure in order to define the required SEL that would trigger potential lesions and, accordingly, determine the combination that would best induce damage to the lice (Table 3).

Table 3. Frequencies and combination of frequencies and amplitudes used.

	Copepodids
500 Hz-2 h-194 SEL	500
500 Hz-4 h-193 SEL	500
500 Hz-4 h-189 SEL	500
350 Hz-2 h-191 SEL	500
350 Hz-2 h-167 SEL	500
350 Hz-2 h-500 Hz-2 h-195 SEL	500
350 Hz-2 h-500 Hz-2 h-191 SEL	500
350 Hz-3 h-192 SEL	500
350 Hz-2 h-500 Hz-1 h-194 SEL	500
Control-152 SEL	500

Sea Lice Specimens

Ten (10) sets of five hundred (n = 500) copepodids from *L. salmonis* were kept (until required for the experiments) in a closed system of natural seawater (at 7–10 °C, salinity 35‰) consisting of plastic tanks with a capacity of 20 L. An air pump facilitated the copepodid movements in the water column.

Individuals were maintained in the tank system until exposure. Several specimens (see below) were used as controls and were kept in the same conditions as the experimental animals until they were exposed to noise.

Sound Exposure Protocol

The results of the previous experiments allowed us to determine the best response from the lice and to choose the corresponding frequencies or combinations of frequencies to be used for further experimentation. Sequential Controlled Exposure Experiments (CEE) were then conducted on copepodids (5 × 500) of *L. salmonis*. Five additional sets of copepodids (5 × 500) were used as control (Table 3). The same sound exposure set up and sacrifice protocol used as in Section Frequency was followed.

2.1.2. Imaging Techniques

The same imaging techniques were used as with previous experiments with cephalopods [17]. Individuals were processed according to routine Scanning (SEM) and Transmission (TEM) electron microscopy procedures.

Light Microscopy (LM)

Previous to preparing the samples for analysis by SEM and TEM procedures, some light microscopy images of live individuals were taken in order to clarify the morphology and location of the sensory setae of the first antenna.

Scanning Electron Microscopy (SEM)

All sets of *L. salmonis* copepodids (control and treatments of exposed sea lice) were used to analyse the lesions after sound exposure.

Fixation was performed in glutaraldehyde 2.5% for 24–48 h at 4 °C. Samples were dehydrated in graded ethanol solutions and critical-point dried with liquid carbon dioxide in a Bal-Tec CPD030 unit (Leica Mycrosystems, Austria). The dried specimens were mounted on specimen stubs with double-sided tape. The mounted samples were gold coated with a Quorum Q150R S sputter coated unit (Quorum Technologies, Laughton, East Sussex, UK) and viewed with a variable pressure Hitachi S-3500N scanning electron microscope (Hitachi High-Technologies Co., Tokio, Japan) at an accelerating voltage of 5 kV in the Institute of Marine Sciences of the Spanish Research Council (CSIC) facilities.

SEM images were used to determine the number of fused setae and to calculate the rate (%) of irregular branching tips of the first antenna that were fused after each treatment.

Transmission Electron Microscopy (TEM)

Ten (10) exposed and ten control *L. salmonis* copepodids were used for this study. Fixation was performed in 2.5% glutaraldehyde-2% paraformaldehyde for 24 h at 4 °C. Subsequently, the samples were osmicated in 1% osmium tetroxide, dehydrated in acetone, and embedded in Spurr. To orient the specimens properly, semithin sections (1 mm) were cut transversally or tangentially with a glass knife, stained with methylene blue, covered with Durcupan, and observed on an Olympus CX41. Ultrathin (around 100 nm) sections of the samples were then obtained by using a diamond knife (Diatome) with an Ultracut Ultramicrotome from Reichert-Jung. Sections were double-stained with uranyl acetate and lead citrate and viewed with a Jeol JEM 1010 at 80 kV. Images were obtained with a Bioscan camera model 792 (Gatan) at the University of Barcelona technical services.

2.2. Sea Trials

Sea trials were performed at an experimental fish farm located in Averøy (Norway). Two isolated test cages were exposed to sound and four cages at different distances from the test cages were used as a control (Figure 2).
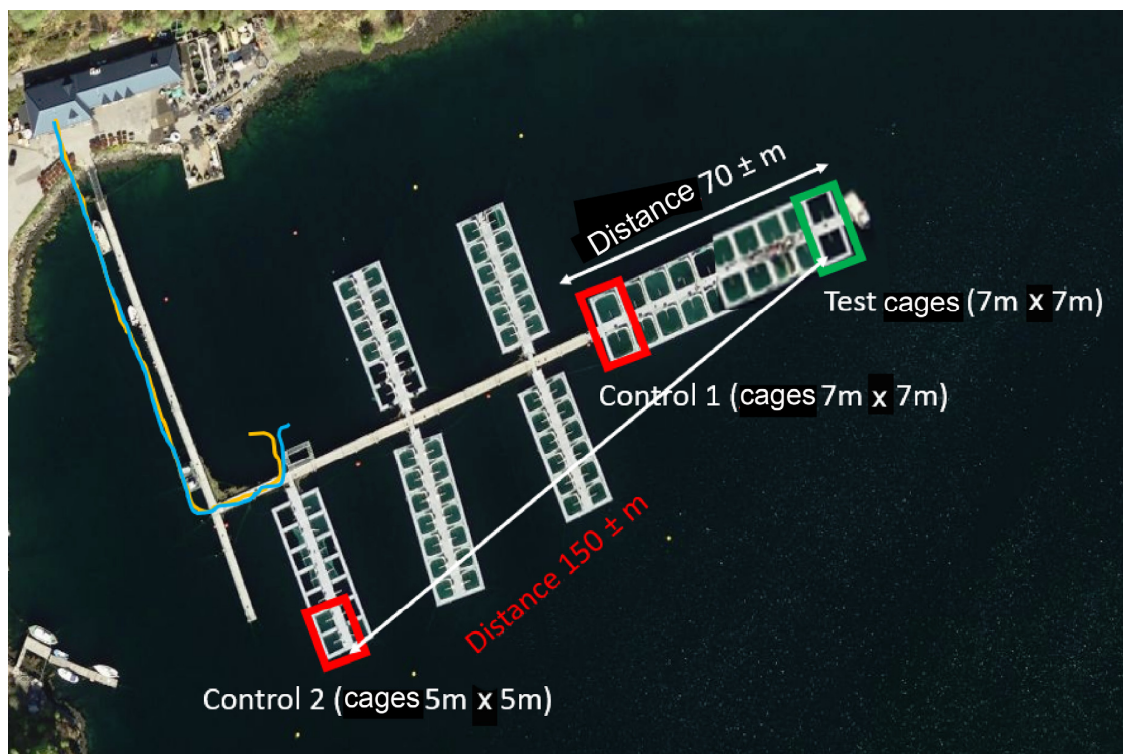

Figure 2. Control and test cages distribution.

2.2.1. Sound Exposure

Sound Exposure Level (SEL)

The protocol refers to the term "Sound Exposure Level (SEL)" as the total cumulative squared sound pressure that an organism is exposed to, expressed in decibels. In other words, it is equivalent to exposing the target organisms to a certain dose of sound. Here, the duration of the exposure represents the cumulative time interval that is necessary to induce lesions.

Sound Pressure Level (SPL)

To expose the target organisms to the necessary SEL, the protocol also refers to the term "Sound Pressure Level (SPL)" as the average sound pressure in a 1 s time interval expressed in decibel, which is produced by an underwater speaker, called a transducer.

Acoustic and Time Parameters for the Sea Trials

The protocol was based on a method and system (Figures 3 and 4) where lice are exposed to continuous acoustic signals over time until a target Sound Exposure Level (SEL) is achieved for the organism: the SEL is chosen at a level that induces sufficient lesions in the sensory organs of the lice to disrupt vital functions necessary for survival, and particularly to detect (and attach) salmon.
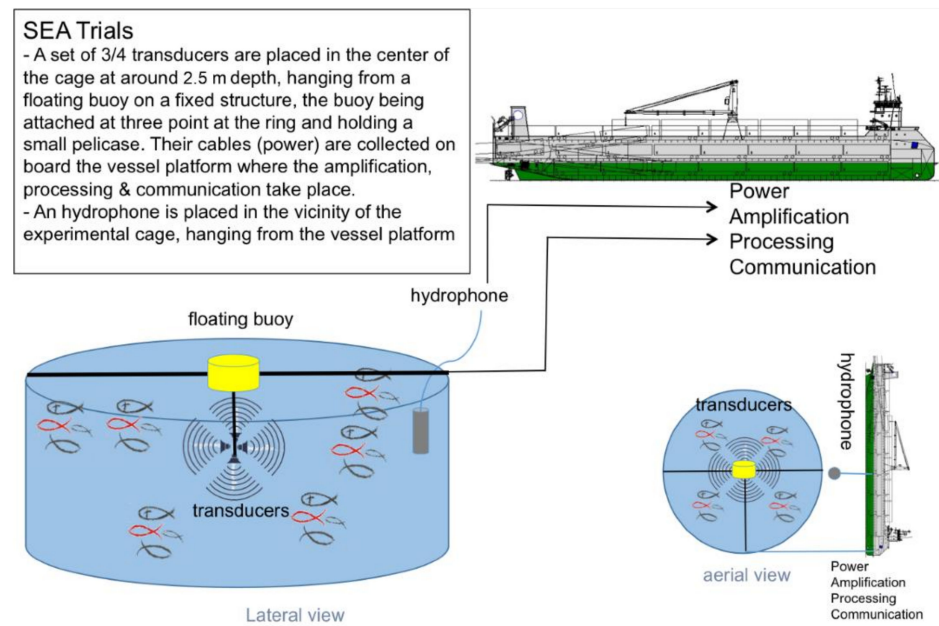
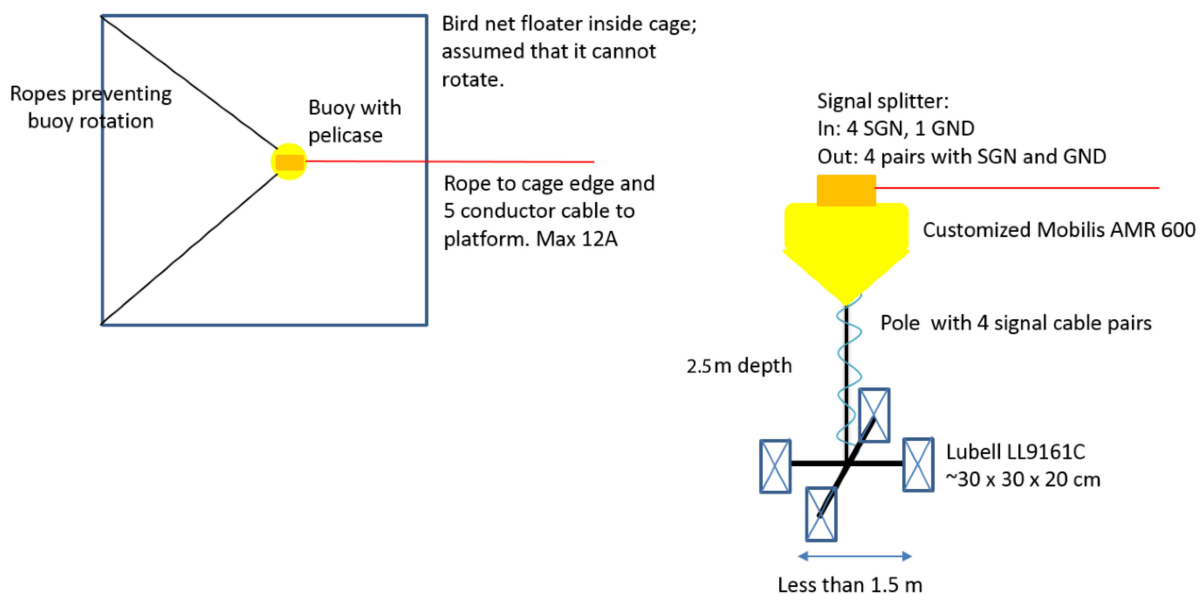**Figure 3.** Sound exposure system.

Figure 4. Drawing of the experimental setup. Note that the depth of the structure that holds the loud speakers was modified along the duration of the experiments. M9 loud speakers were lowered to −5 m.

Based on the output of the previous laboratory experiments (see Section 3, Results) where the lice showed sensitivity to a rather broad range of frequencies (and particularly to continuous exposure to individual 350 Hz and 500 Hz signals) during, respectively, a cumulative cycle of 2 h and 1 h, this combination was initially played back every 4 h (Figure 5). Due to the presence of continuous free-swimming lice from external sources, it was decided to increase the exposure time as well as the SPL at one cage so that the required SEL could be reached faster (see below).
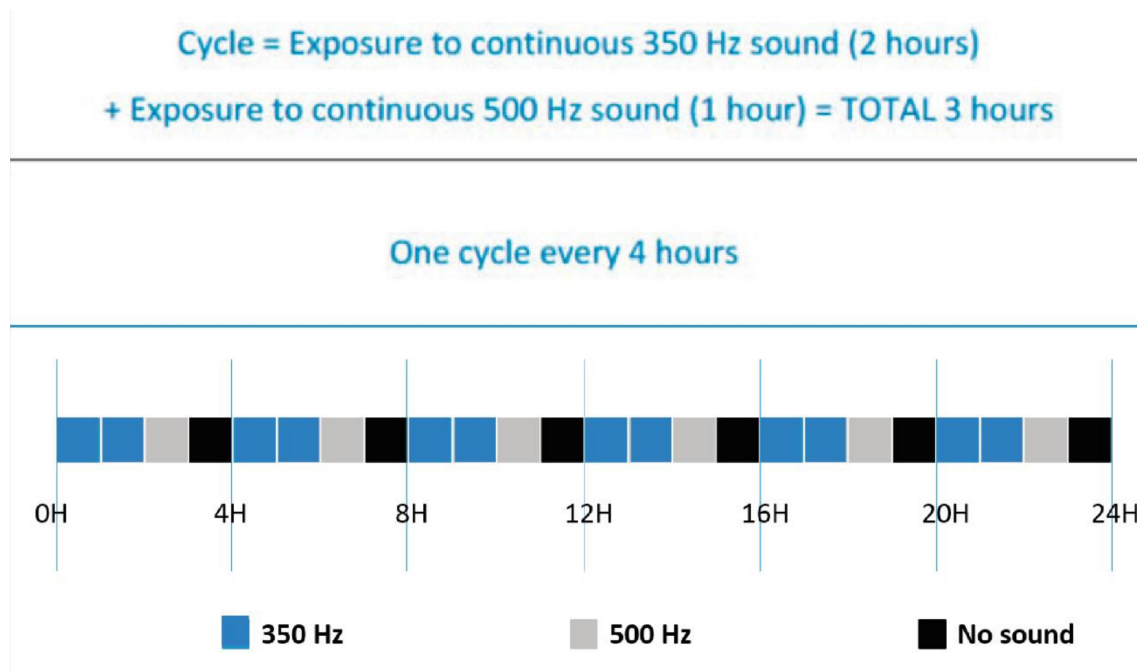

Figure 5. Sound exposure protocol. Note that this cycle was modified along the duration of the experiments favouring the exposure to 500 Hz to produce higher SPL.

Hardware

Under the sea trial protocol, the system and method included producing the sounds using calibrated transducers capable of reproducing sound covering the essential part of the sensitivity range for the lice, particularly from 300 Hz to 600 Hz. The transducers had a source level of at least up to 160 dB re 1 μPa^2 at 1 m for individual frequencies and 180 dB re 1 μPa^2 at 1 m for each selected third octave band. The transducers were driven by amplifiers that could reach the required voltages to reach these levels. Typical peak voltage levels were below 100 V. The sound production system was calibrated as a whole and for each individual frequency.

Calibrated hydrophones recorded the acoustic pressure in a given frequency range with maximum sound pressure levels at least up to 180 dB re $1\mu Pa^2$ without saturation. The hydrophone system was arranged to provide digitized data to a sound exposure control system.

2.2.2. Scanning Electron Microscopy (SEM)

Ten (10) exposed and ten control *L. salmonis* for each pre-adult and adult stage were used for this study. The fish in sea conditions were naturally exposed to lice infestation. The lice specimens were collected after two weeks from the start of the sound exposure experiments from the fishes in the cages and processed immediately for the analysis. Individuals were processed according to routine SEM procedures (See Section Scanning Electron Microscopy (SEM)).

2.2.3. Transmission Electron Microscopy (TEM)

Ten (10) exposed and ten control *L. salmonis* for each chalimus, pre-adult and adult stage were used for this study. The specimens were collected after three and six weeks (chalimus), after six weeks (adults and pre-adults) from the start of the sound exposure experiments, and from the fishes in the cages and were processed immediately for the analysis. Individuals were processed according to routine TEM procedures (See Section Transmission Electron Microscopy (TEM)).

3. Results

3.1. Laboratory Experiments

3.1.1. *L. salmonis* Copepodids Sensory Setae Morphology

Copepodids (length 0.7 ± 0.01; width 0.2 ± 0.01) (Figure 6) present 10 pairs of setules arranged symmetrically about the medial longitudinal axis (6 pairs of simple setules, 4 pairs bifurcates) on the dorsal shield of the cephalothorax and 2 simple setules near the base of the rostrum.
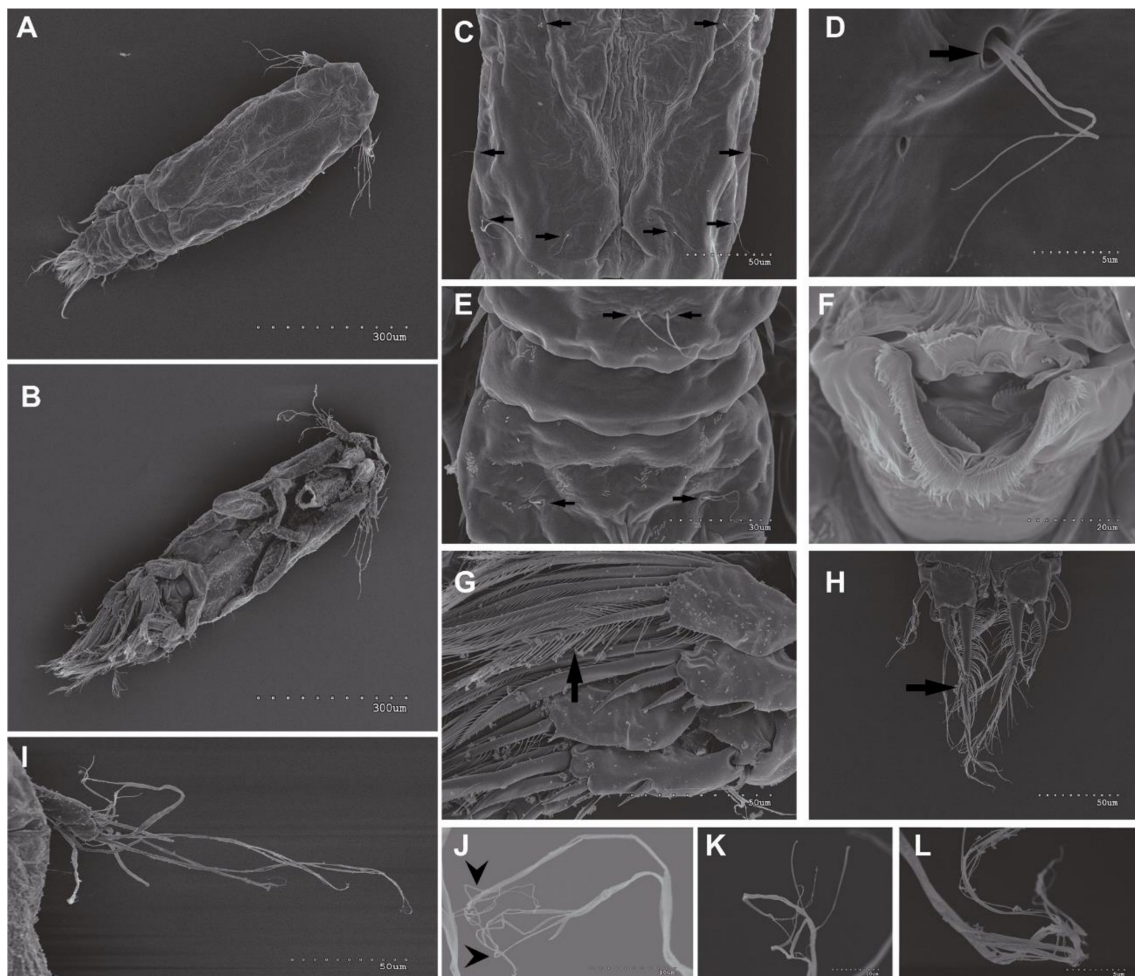

Figure 6. SEM. Copepodid setae morphology. Control animals: (**A**) Dorsal and (**B**) Ventral view of a *L. salmonis* copepodid. (**C**) Cephalothorax dorsal view showing some paired setae distributed along the body (arrows). (**D**) Detail from C shows the structure of a birrame setae (arrow). (**E**) Dorsal view of the abdomen showing some paired setae (arrows). (**F**) Mouth of the copepodid. (**G**) Ventral arms showing pinnate setae (arrow). (**H**) Caudal ramus showing the distal setae (arrow). (**I**) First antenna. The irregular branching tips are visible (arrowheads). (**J–L**) Detail of the first antenna setae showing their irregularly branching tips. Scale bar: (**A,B**) = 300 µm; (**C,G,H,I**) = 50 µm; (**E**) = 30 µm; (**F**) = 20 µm; (**J,K**) = 10 µm; (**D,L**) = 5 µm.

The first antenna (Figure 6) presents a proximal segment with 3 unramed setae and a distal segment with 5 setae with irregularly branching tips, 7 unramed setae, and 1 aesthete. The second antenna exhibits 3 segments with a spiniform process.

The 3 thoracic legs (Figure 6) present plumose setae, semipinnate setae, pinnate setae, spines, spiniform process, and fine setules. Caudal ramus (Figure 6) shows both short and long pinnate setae and aesthete.

3.1.2. Ultrastructural Analysis of Copepodids Setae after Noise Exposure

Ultrastructural changes took place on *L. salmonis* copepodid setae following acoustic exposure. In the control animals, the first antenna presented completely free setae with irregularly branching tips on the distal segment (Figure 7A–D). All the exposed copepodids presented different degrees of fusion of the irregularly branching tips of the setae on the distal segment of the first antenna (Figure 7E–T).
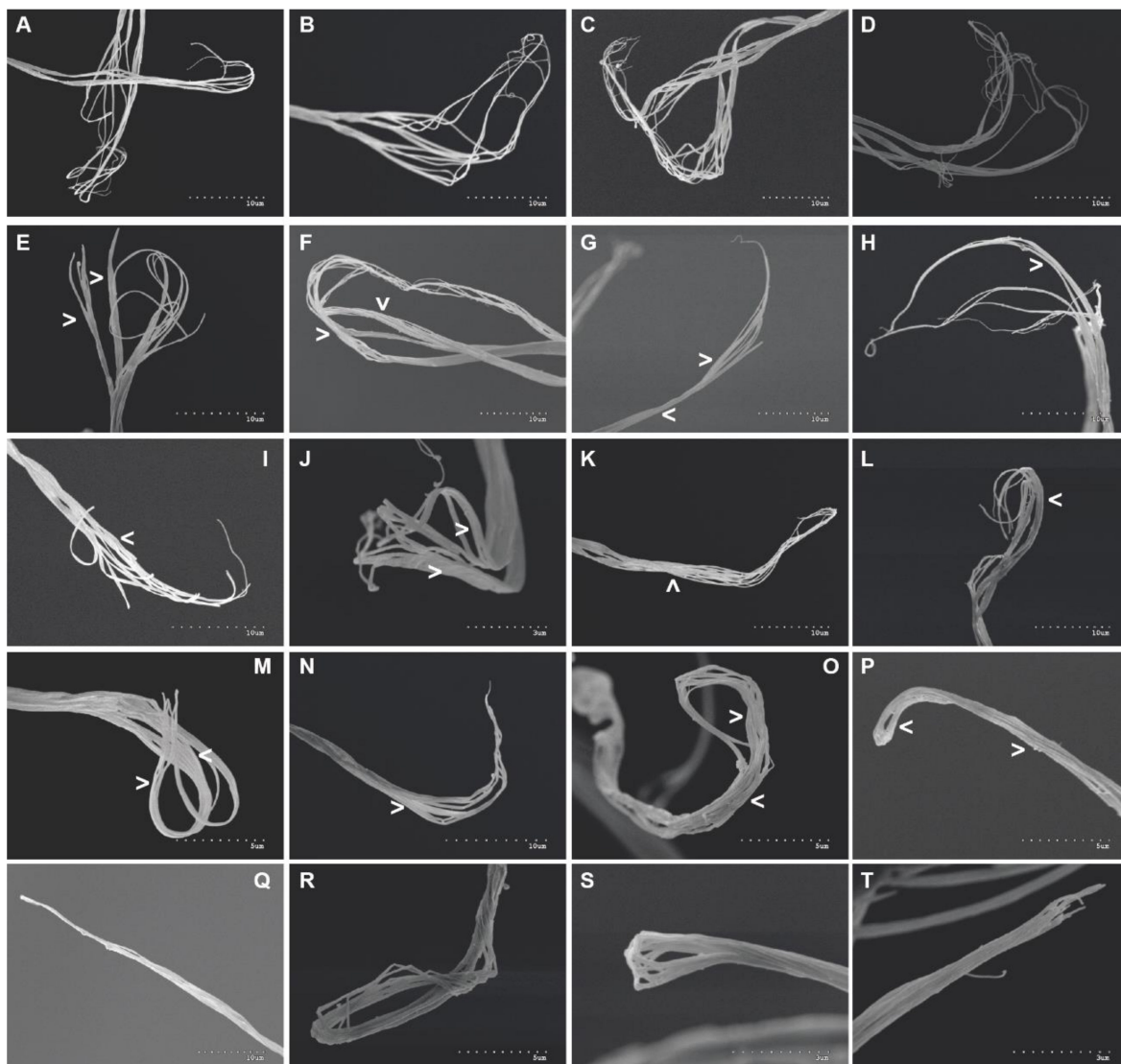

Figure 7. SEM: (**A**) *L. salmonis* copepodids. Setae on distal segment of first antenna; (**A–D**) Normal setae on control animal. The tips on the setae distal segments are entirely free (not fused); (**E–H**) Different views of exposed animals showing fusion (arrowheads) on the basal segment of the setae on the distal segment of the first antenna; (**I–N**) Different views of exposed animals showing the almost entirely fused (arrowheads) distal segment of the first antenna; (**O–T**) Different views of exposed animals showing completely fused distal segment of the first antenna. Scale bar: (**A–I,K,L,N,Q**) = 10 μm; (**M,O,P,R**) = 5 μm; (**J,S,T**) = 3 μm.

3.1.3. Exposure Parameters vs. Lesions

Frequency

After sound exposure and the analysis of the first antenna setae of the sea lice, we found maximum fusion at 350 Hz (95.5%). However, with frequencies between 300 Hz and 550 Hz, we achieved a percentage of setae fusion higher than 90% (Figure 8).
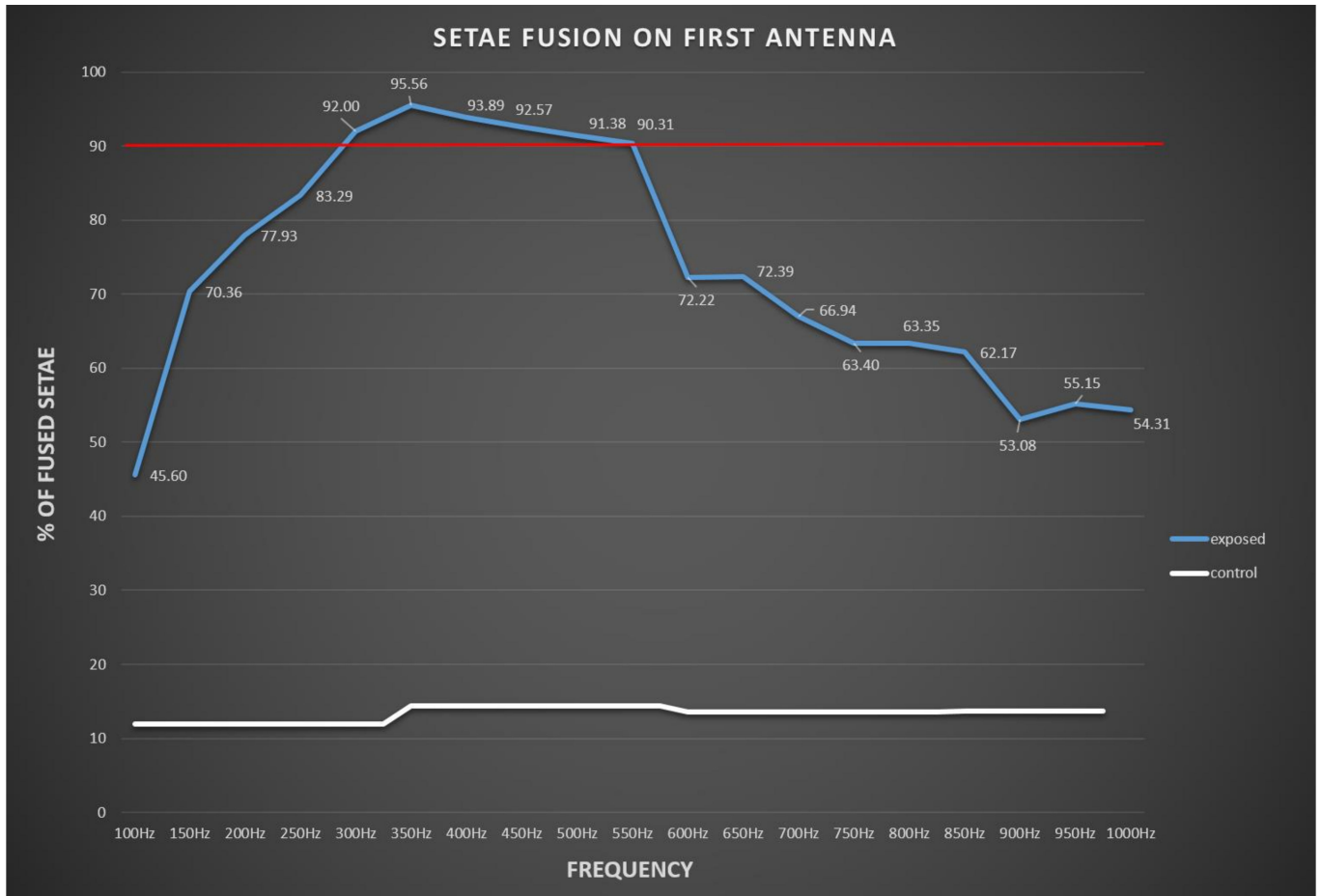

Figure 8. Setae fusion on sea lice first antenna (%) in function of frequency. 350 Hz achieved the maximum percentage of setae fusion. Between 350 Hz and 550 Hz the fusion percentage was higher than 90% (red bar).

After exposure to combinations of frequencies that previously had achieved the maximum fusion and the analysis of the first antenna setae of the sea lice, we found that 350 Hz–450 Hz and 350 Hz–550 Hz were the two combinations that achieved the maximum percentage of setae fusion (95.2%) (Figure 9).

We appointed that there was not a significant increase in the level of fusion with the combination of two frequencies.
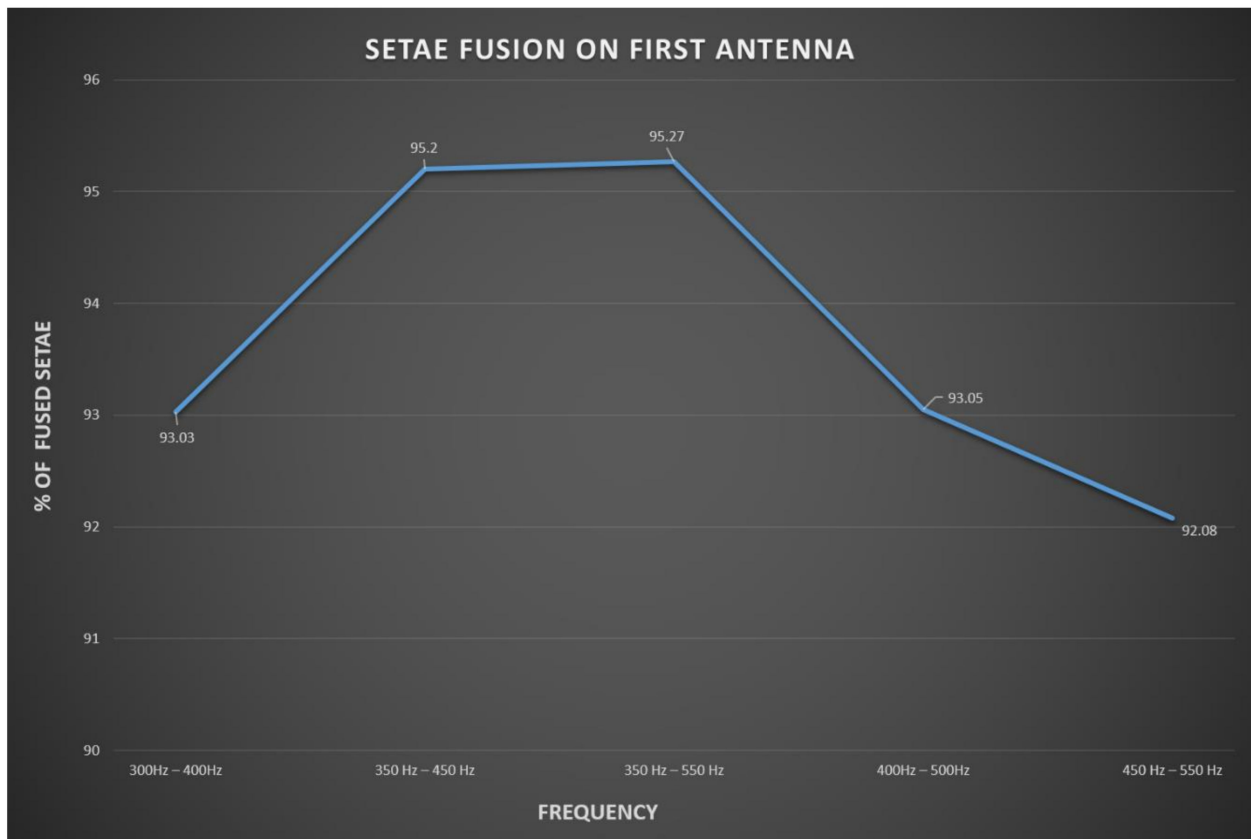
Figure 9. Setae fusion on sea lice first antenna (%) in function of frequency combinations of 350 Hz–450 Hz and 350 Hz. 550 Hz are the combination that achieve the maximum percentage of setae fusion (95.2%).

Amplitude

We found maximum setae fusion with the combination of 350 Hz-2 h-65 V and 500 Hz-2 h-65 V (93.02%). Other combinations (e.g., 350 Hz-2 h-65 V and 500 Hz-1 h-65 V, 350 Hz-3 h-65 V) achieved a percentage of setae fusion higher than 90% (Table 4).

Table 4. Setae fusion on sea lice first antenna (%) in function of frequency, time, and level of exposure in our tank conditions.

	% Fused Antenna
350 Hz-2 h-191 SEL	89.68
350 Hz-2 h-167 SEL	70.17
500 Hz-2 h-194 SEL	84.75
500 Hz-4 h-193 SEL	87.91
500 Hz-4 h-189 SEL	77.58
350 Hz-2 h-500 Hz-2 h-195 SEL	93.02
350 Hz-2 h-500 Hz-1 h-194 SEL	90.11
350 Hz-3 h-192 SEL	92.13
350 Hz-2 h-500 Hz-2 h-191 SEL	83.32
Control-152 SEL	12.89

3.1.4. Determination of Ultrastructural Lesions in Inner Tissues of Sea Lice Copepodids

Sound exposure affected the nervous system and A/B cells, which are responsible for the precursor secretions of the frontal filament. The lesions present in all the samples of exposed sea lice copepodids (but not in any of the control animals) were characterized by an exuberant accumulation of dark material and by cell cytoplasm vacuolization (Figures 10 and 11). These pathological features suggest the involvement of massive autophagy processes.
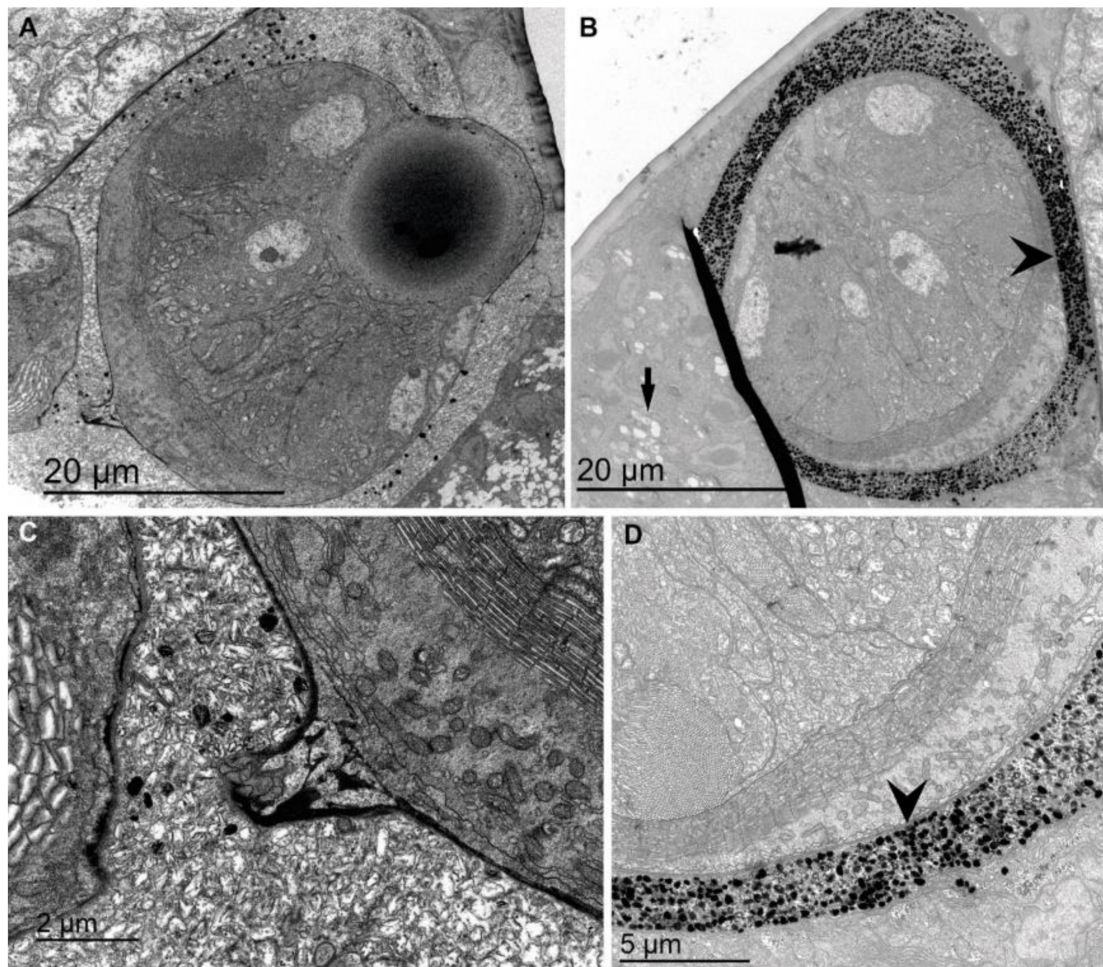
Figure 10. TEM. Sagittal section of the copepodid anterior cephalotorax showing the copepodid eye: (**A**,**C**) Control copepodid; (**B**,**D**); Exposed copepodid. (**A**) In control animals the dark inclusions around the eye are scarce. (**B**) In exposed copepdids a large amount of dark inclusions are visible in the axons of the central nervous system surrounding the eye (arrowhead). Vacuolization is visible on the tissue surrounding the eye (arrow); (**C**) Detail of A showing the optic nerve. Note the low quantity of dark inclusions around the eye; (**D**) Detail from B. Arrowhead point to the large amount of dark inclusions. Scale bar: (**A**,**B**) = 20 μm; (**D**) = 5 μm; and (**C**) = 2 μm.
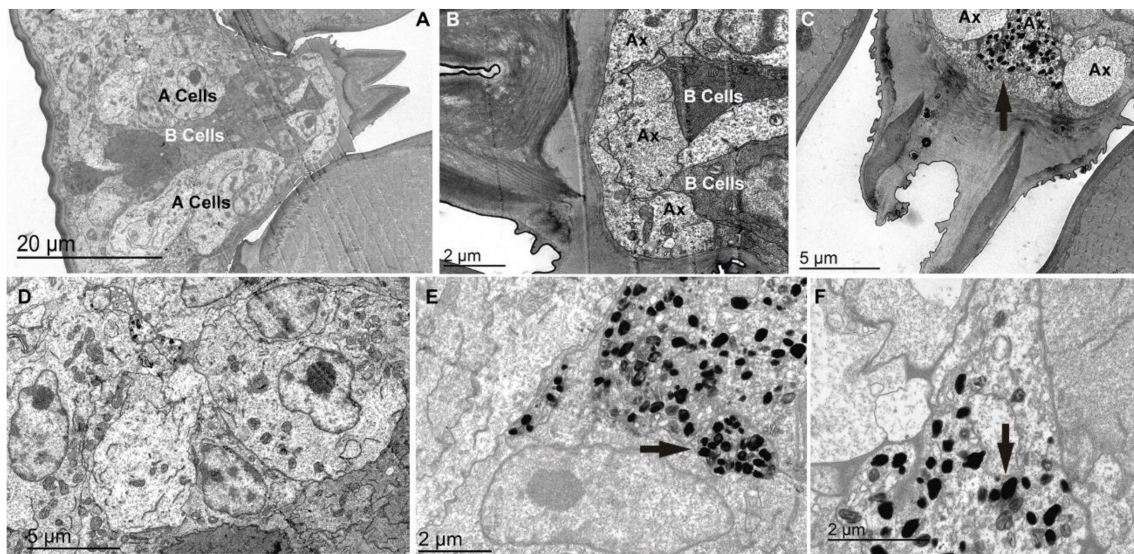
Figure 11. TEM. Frontal medial section of the copepodid anterior cephalotorax showing A and B Cells involved in Frontal Filament production: (**A,B,D**) Control; (**C,E,F**) Exposed: In control animals A and B cells do not show inner dark inclusions. (**B**) Axons sited next to A and B cells present normal aspect. (**C**) In exposed copepodids dark inclusions are visible in the axons of the nervous system (arrow). (**D**) Normal aspect of cells without dark inclusions. (**E,F**) Dark inclusions in the cells of exposed copepodids (arrows). Scale bar: (**A**) = 20 μm; (**C,D**) = 5 μm; and (**B,E,F**) = 2 μm.

3.2. Sea Trials

3.2.1. *L. salmonis* Adult and Pre-Adult Sensory Setae Morphology

In adult and pre-adult specimens (length 9.9 ± 1; width 4.5 ± 0.2), the first antenna (Figure 12) presents a proximal segment with 27 setae (25 pinnate on ventral and 2 unramed on dorsal surface) and a distal segment bearing 1 seta on posterior margin and 11 setae and 2 aesthetes at apex. Some setae are visible on maxilas too. The five pairs of legs present unramed setae, pinnate setae, spines and rows of simple setules. Caudal ramus shows distal setae with distinctly inflated bases that are relatively short.
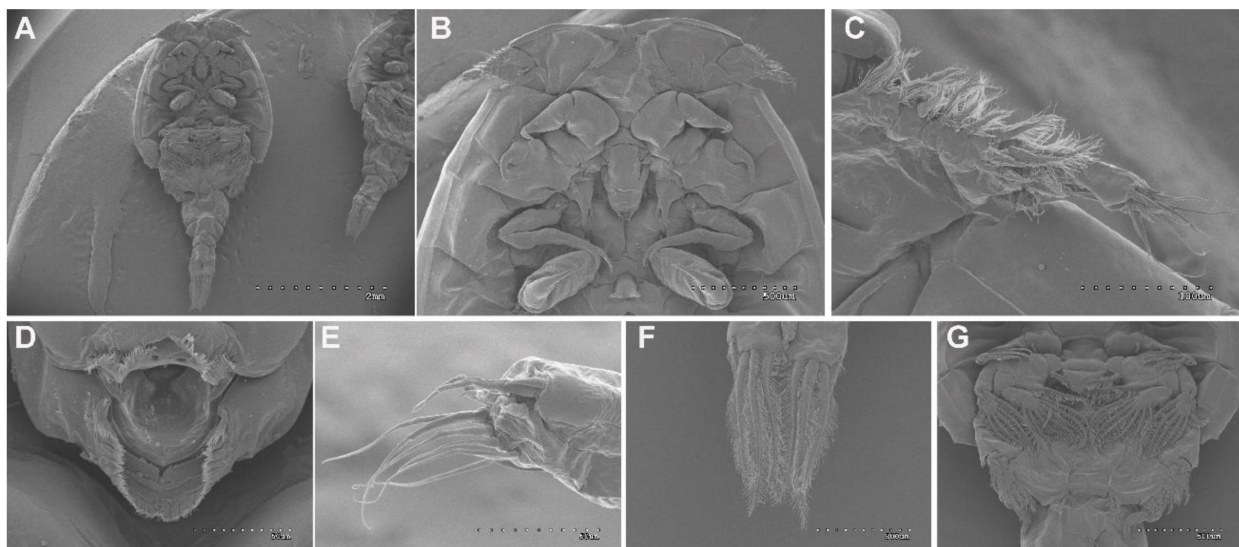

Figure 12. SEM. Adult and pre-adult *L. salmonis* morphology. Control animals: (**A**) Ventral view of the whole body of a pre-adult; (**B**) Ventral anterior view of an adult; (**C**) First antenna of an adult *L. salmonis*; (**D**) Mouth of a pre-adult; (**E**) Distal segment of the first antenna of *L. salmonis* adult; (**F**) Caudal ramus showing the distal setae; (**G**) Ventral arm showing the distribution of the pinnate setae. Scale bar: (**A**) = 2 mm; (**B,D,G**) = 500 μm; (**F**) = 300 μm; (**C**) = 100 μm; and (**E**) = 50 μm.

3.2.2. Ultrastructural Analysis of Pre-Adult and Adult First Antenna Setae after Noise Exposure

Ultrastructural changes took place on setae in adults and pre-adults of *L. salmonis* following acoustic exposure. Damaged setae were either extruded, completely missing, or presented flaccid, fused, or missing sensory hairs.

After two weeks of sound exposure (Figure 13B,D,E,G and Figure 14B–E) in comparison with the same tissues from control animals (Figures 13A and 14A), damage was observed on the first antenna setae. The setae of the proximal segment of the first antenna presented sensory hairs flaccid, fused or showed blebs. Some setae had lost part of the sensory hairs. Sometimes the setae had lost their rigidity and appeared unstructured and almost empty. Some animals presented setae partially or completely ejected above the antenna surface (Figures 13G and 14E).
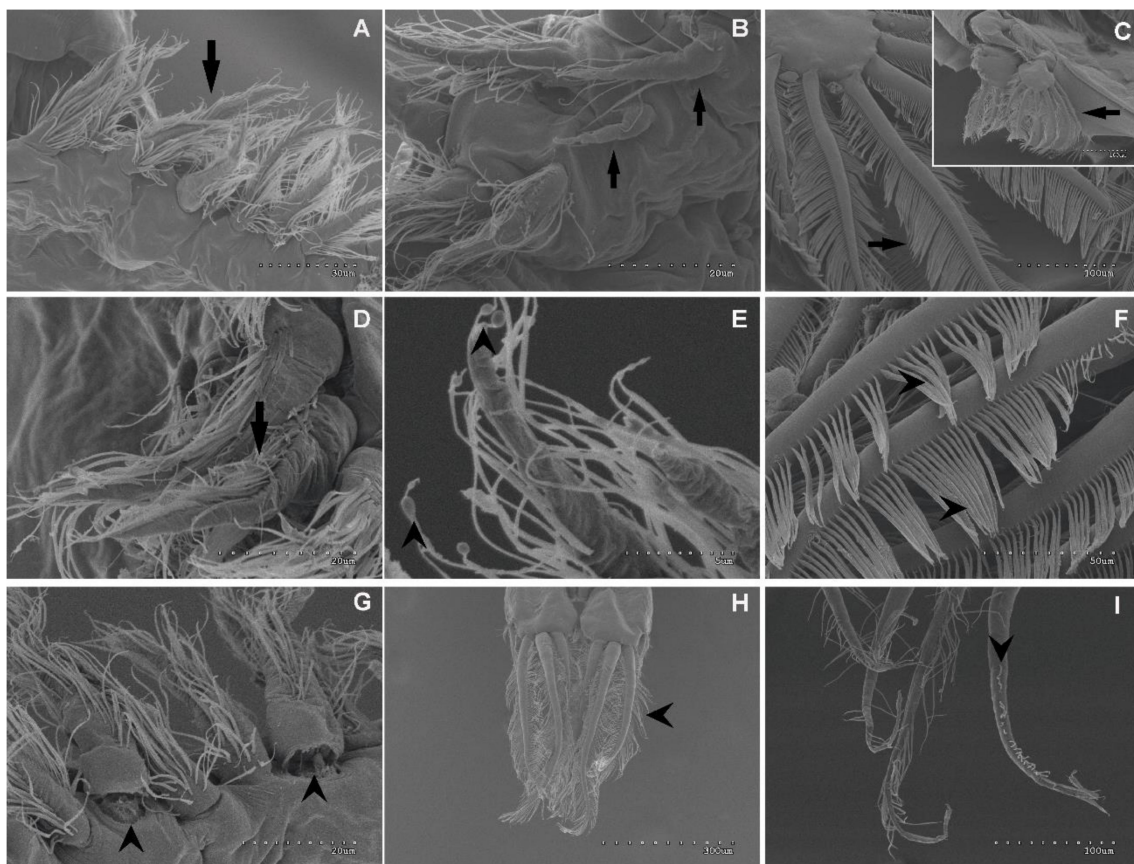

Figure 13. SEM. Pre-adult *L-salmonis* setae on proximal segment of first antenna: (**A,C,H**) Control animals; (**B,D–G,I**) animals after 2 weeks of sound exposure on sea trials. (**A**) Image of healthy setae bearing organized sensory hairs (arrow). (**B**) Setae showing flaccid or fused sensory hairs. Some of them have almost entirely lost the sensory hairs (arrows). (**C**) Pinnate setae on ventral arms presenting normal aspect (arrow). Insert in (**C**), lateral fraction of ventral arms presenting sensory hairs with normal aspect (arrow). (**D**) Section of proximal segment of the first antenna showing all the setae bearing bend and flaccid sensory hairs (arrow). (**E**) Sensory hairs showing blebs (arrowheads). (**F**) Pinnate setae on ventral arms are fused. (**G**) Setae partially ejected (arrowheads) above the antenna surface. (**H**) Normal aspect of the sensory hairs in the distal setae on caudal ramus. (**I**) Caudal ramus has partially lost the sensory hairs. Scale bar: (**H**) = 300 μm; (**C,I**); Insert in (**C**) = 100 μm; (**F**) = 50 μm; (**A**) = 30 μm; (**B,D,G**) = 20 μm; and (**E**) = 5 μm.
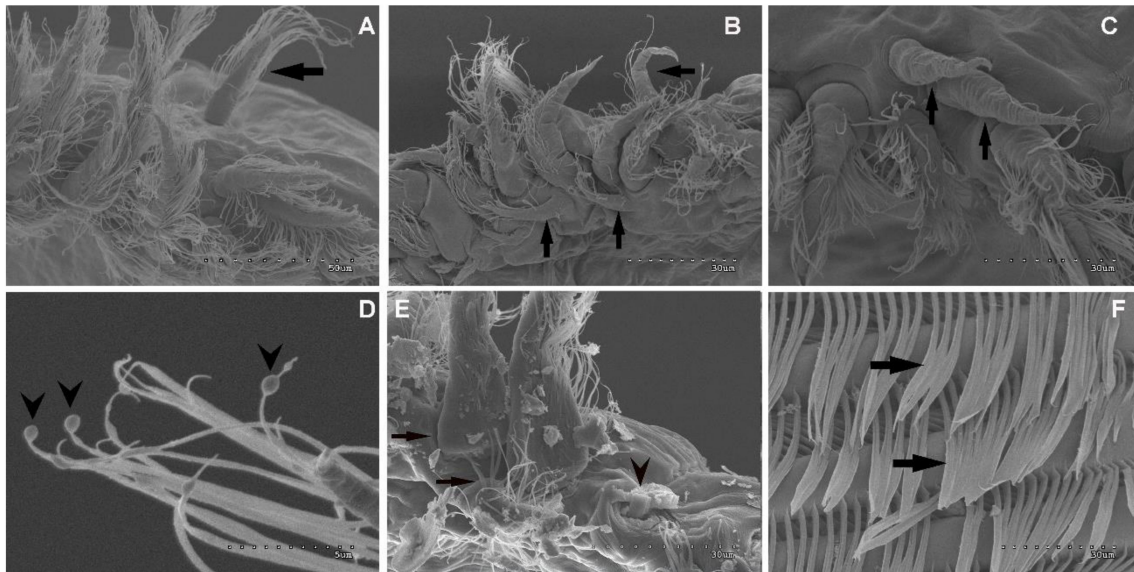
Figure 14. SEM. Adult *L. salmonis* setae on proximal segment of first antenna: (**A**) Control animals; (**B–F**): animals after two weeks of sound exposure on sea trials. (**A**) Image of healthy setae bearing organized sensory hairs (arrow). (**B**) Setae showing flaccid or fused sensory hairs. Some of them have almost lost totally the sensory hairs (arrows). (**C**) Some of the setae have almost lost totally the sensory hairs (arrows). (**D**) Sensory hairs showing blebs (arrowheads). (**E**) Two setae are partially (arrows) or totally ejected (arrowhead) above the antenna surface. (**F**) Pinnate setae on ventral arms are fused (arrows). Scale bar: (**A**) = 500 μm; (**B,C,E,F**) = 30 μm; and (**D**) = 5 μm.

In some specimens, in addition to the lesions on the first antenna, we found some effects on setae located in other positions. The arms showed sections of different lengths of fused pinnate setae (Figures 13F and 14F). Some specimens presented loss of sensory hairs or broken bases of the distal setae on caudal ramus (Figure 13I).

3.2.3. Ultrastructural Analysis of Chalimus, Pre-Adult and Adult *L. salmonis* Inner Tissues after Sound Exposure

Sound effects were observed in chalimus, pre-adult, and adult stages in comparison with the control animals. All noise-exposed individuals presented a similar variety of ultrastructural changes in cells of the inner tissues surrounding the eyes (in chalimus, specifically in cells involved in frontal filament production, namely A and B cells) and in axons of neurons around the eyes. In cell cytoplasm, ultrastructural changes were essentially a massive accumulation of dark inclusions (including ribosomes), the presence of numerous large double-membrane bounded autophagic vacuoles and of numerous lysosomes, and vacuolization of the cell cytoplasm (Figures 15–20). In addition, some B cells showed a deformed cell nucleus and chromatin compaction into the nucleus (Figure 15).

In the axons of neurons around the eyes, prominent ultrastructural changes were the presence of both abundant double-membrane-bounded autophagic vacuoles and myelin-like formations (Figures 15–18 and 21), and the accumulation of lysosomes at different stages of evolution (Figures 19 and 21). Large areas of empty cytoplasm (Figures 16–18, 20 and 21) and the accumulation of dark inclusions including ribosomes were also a common feature in these nervous cells (Figures 15, 17 and 18).
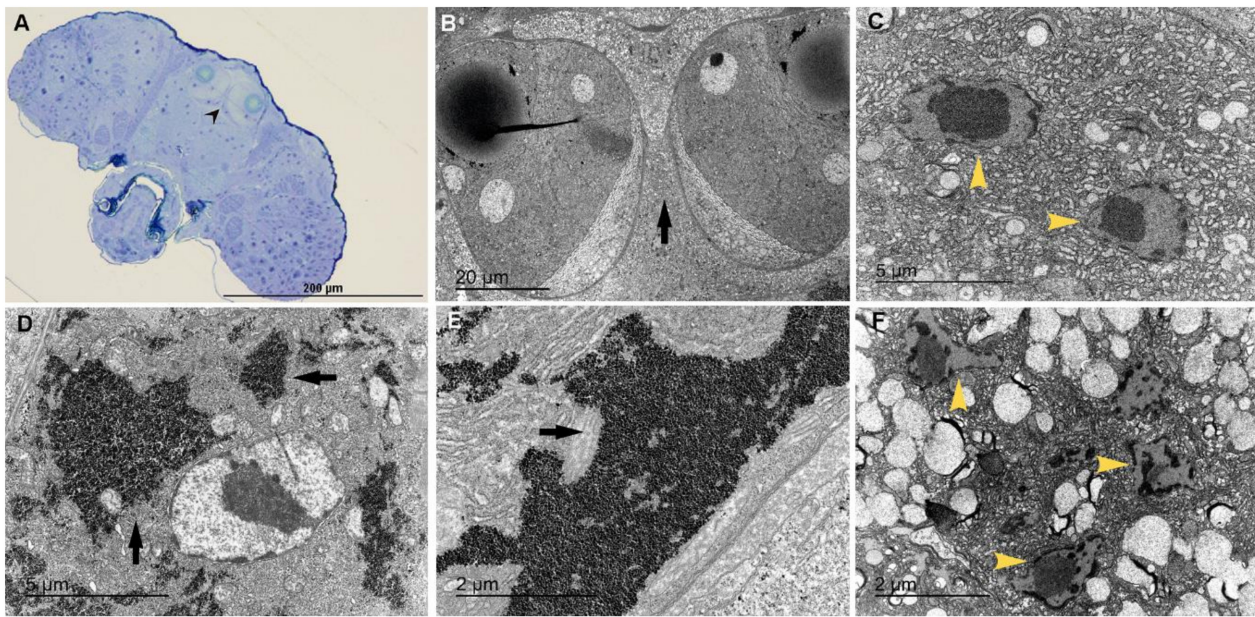
Figure 15. (**A**) Light microscopy; (**B**–**F**) TEM. Frontal medial section of a chalimus stage of sea lice; (**A**–**C**) Control specimens; (**D**–**F**) 3 weeks exposed specimens. (**A**) In light microscopy images of control animals there are not specially stained areas (corresponding to dark inclusions in TEM). Arrowhead shows the eyes. (**B**) Eyes of a control animal. The axons of the central nervous system surrounding the eye did not show dark inclusions (arrow). (**C**) Normal B cells nucleus (yellow arrowheads) in a control animal. (**D**) Dark inclusions in A cell cytoplasm are visible (arrows). (**E**) A large section of the cytoplasm of A cells are filled with ribosomes (dark inclusions, arrow). (**F**) By comparison to C, the B cell nuclei on exposed animals presented irregular shapes and chromatin compaction (yellow arrowheads). Scale bar: (**A**) = 200 μm; (**B**) = 20 μm; (**C**,**D**) = 5 μm; (**E**,**F**) = 2 μm.
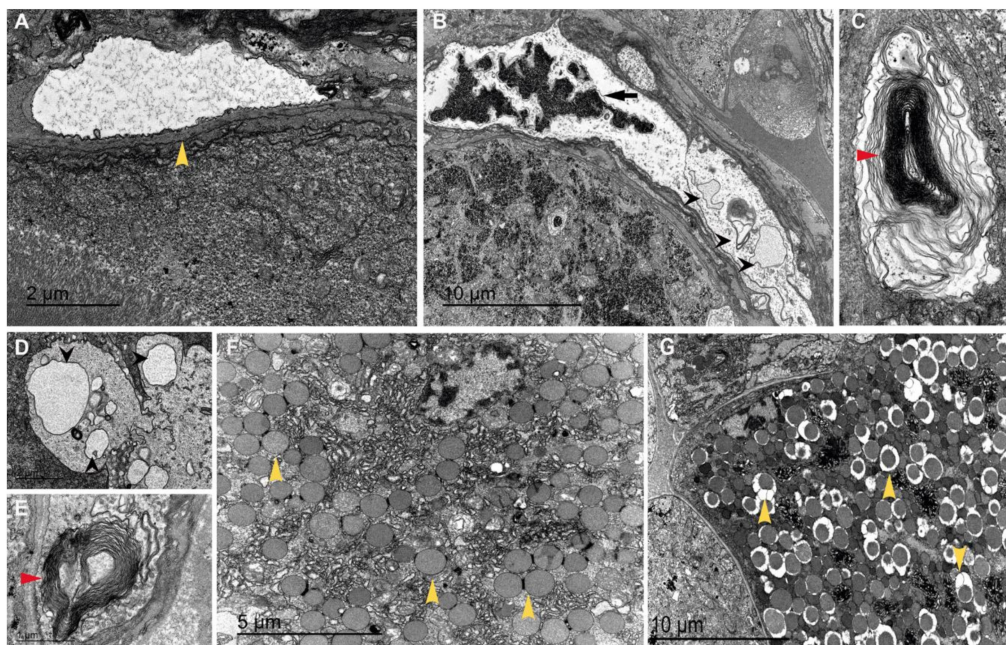

Figure 16. TEM. Frontal medial section of a chalimus anterior cephalothorax: (**A**,**F**) Control specimens; (**B**–**E**,**G**) 3 weeks exposed specimens. (**A**) There are no dark inclusions visible in the central nervous system axons (yellow arrowhead) neighbours to the eye. (**B**) One axon of the central nervous system shows ribosome accumulation (arrow) and presence of double-membrane-bounded autophagic vacuoles (arrowheads). (**C**,**E**) "Myelin-like formations" (red arrowhead). (**D**) Double-membrane-bounded autophagic vacuoles (arrowheads). (**F**) Normal aspect of the tissue located next to the B cells. (**G**) the tissue shows a process of vacuolization (yellow arrowheads). Scale bar: (**B**,**G**) = 10 μm; (**F**) = 5 μm; (**A**,**C**,**D**) = 2 μm; (**E**) = 1 μm.
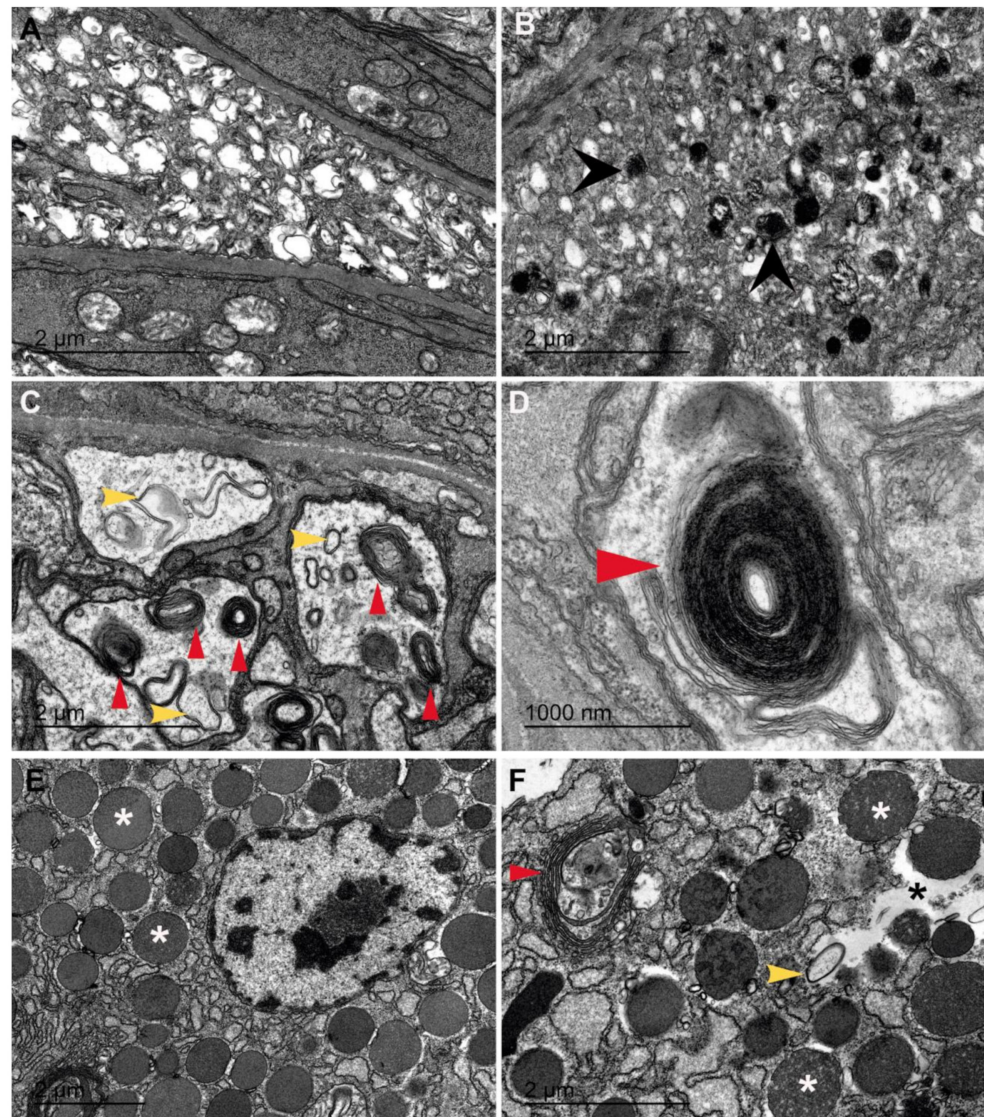
Figure 17. TEM. Frontal medial section of a chalimus anterior cephalothorax: (**A,E**) Control specimens; (**B,C,D,F**) Six weeks exposed specimens. (**A**) Normal aspect of the central nervous system between the two eyes. (**B**) By comparison to A, large dark inclusions (black arrowheads) are visible in the central nervous system between the two eyes. (**C**) "Myelin-like formations" (red arrowheads) and double-membrane-bounded autophagic vacuoles (yellow arrowheads) are present in axons. (**D**) Detail of "myelin-like formations" in an axon (red arrowhead). (**E**) Normal lysosomes (white asterisks) next to the B cell nuclei. (**F**) Some degraded lysosomes (white asterisks) are visible in a B cell of an exposed animal. "Myelin-like formations" (red arrowhead) and autophagic vacuoles (yellow arrowhead) are present. Note the empty cytoplasm in some areas of the tissue (black asterisks). Scale bar: (**A–C,E,F**) = 2 μm; (**D**) = 1000 nm.
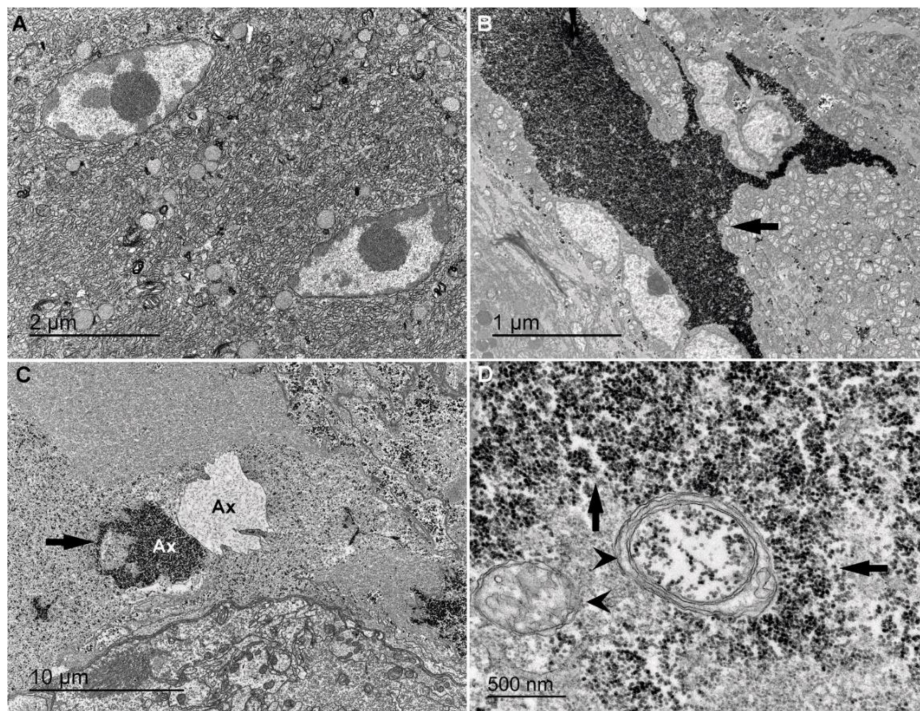
Figure 18. TEM. Frontal medial section of a pre-adult anterior cephalothorax showing tissues located around the eyes: (**A**) Control specimens; (**B,C,D**) Exposed specimens. (**A**) Normal aspect of cells in tissue surrounding the eyes. No dark inclusions are visible. (**B**) A large section of the cytoplasm is filled with ribosomes (dark inclusions, arrow). (**C**) One axon filled with dark inclusions (arrow) is adjacent located to one normal axon. (**D**) In the cytoplasm of an axon note the accumulation of ribosomes (dark inclusions, arrows) and the presence of autophagic vacuoles (arrowheads). Scale bar: (**C**) = 10 μm; (**A**) = 2 μm; (**B**) = 1 μm; (**D**) = 500 nm.
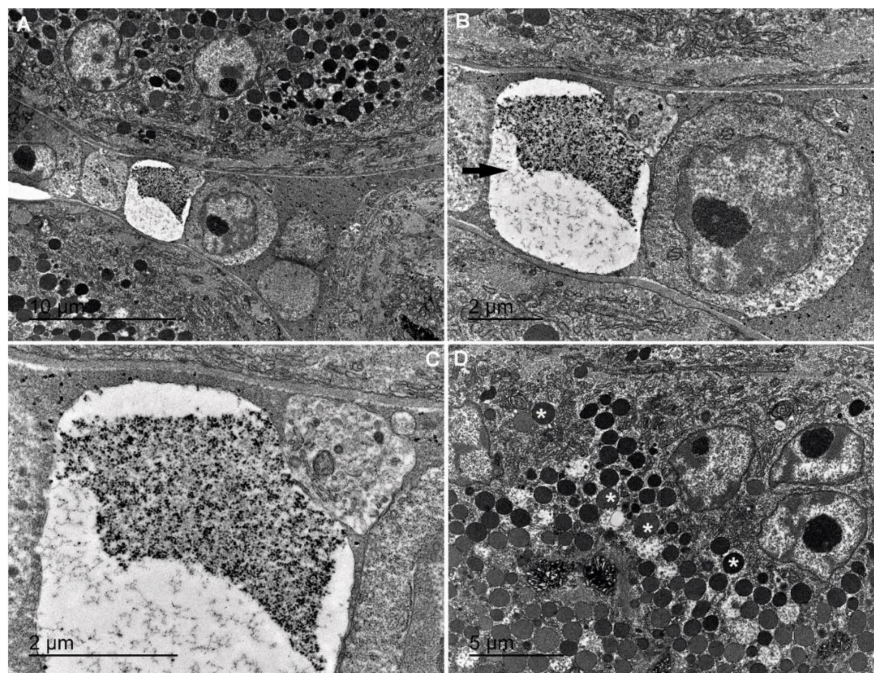

Figure 19. TEM. Frontal medial section of an exposed pre-adult anterior cephalothorax. Exposed animal: (**A**) General view of a section of tissue showing different features on sound exposed cells (Details in **B–D**); (**B**) Two adjacent cells are visible. On the right a normal cell shows its nucleus with inner nucleolus. On the left (arrow) a sound affected cell shows organelles destroyed by an enzymatic process; (**C**) Detail from (**B,D**), presence of very dark lysosomes (asterisks). Scale bar: (**A**) = 10 μm; (**D**) = 5 μm; and (**B,C**) = 2 μm.
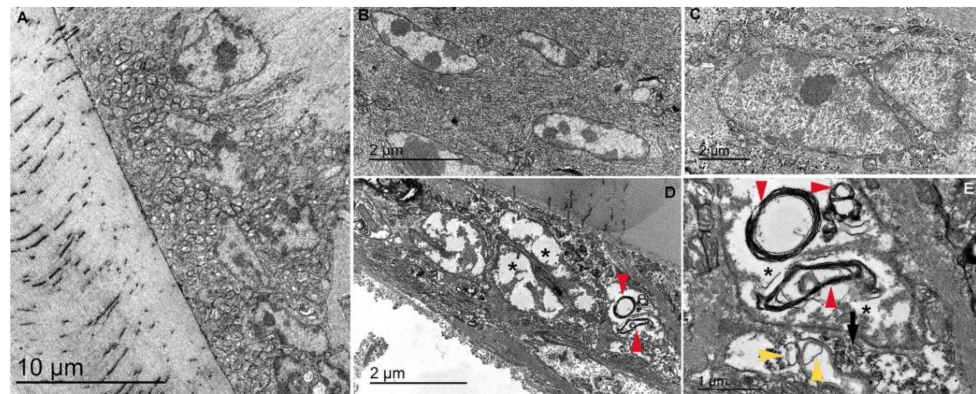
Figure 20. TEM. Sagittal section of adult sea lice anterior cephalothorax: (**A–C**) control animals; (**D,E**) Exposed animals; (**A–C**) No abnormal features are visible. (**D**) Cells present large empty areas in the cytoplasm (asterisks). Red triangles point to "myelin-like formations". (**E**) Detail from D. Note the double-membrane-bounded autophagic vacuoles (yellow arrowheads), the empty areas of cytoplasm (asterisk), the "myelin-like formations" (red arrowheads) and ribosome accumulation (arrow). Scale bar: (**A**) = 10 μm; (**B–D**) = 2 μm; (**E**) = 1 μm.
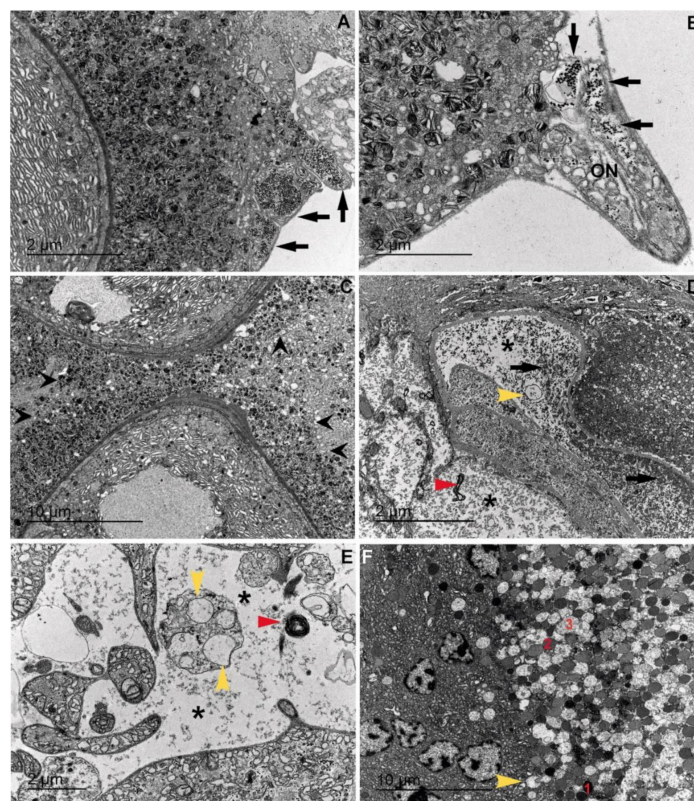

Figure 21. TEM. Frontal medial section of exposed adult anterior cephalothorax showing tissues located around the eye. (**A**) Arrows point to cells of the central nervous tissue filled with dark inclusions (ribosomes). (**B**) Detail from the optic nerves (ON) showing ribosome accumulation (arrows). (**C**) The axons of the central nervous system between the two eyes present some large dark inclusions (arrowheads). (**D,E**) Cells of the central nervous system shows autophagic vacuoles (yellow arrowheads), empty areas of cytoplasm (asterisks), "myelin-like formations" (red triangles) and ribosome accumulation (arrows). (**F**) The large amount of lysosomes type 3 suggest the evolution sequence of lysosomes going from the darkest (1) to lightest (3) appearance probably linked to sustained autophagy. Yellow arrowhead points to a type 3 lysosome releasing their inner content to a next autophagosoma. Scale bar: (**C,F**) = 10 μm; (**A,B,D,E**) = 2 μm.

4. Discussion

The sea louse *L. salmonis* causes millions of dollars in commercial losses to the salmon aquaculture industry globally. It reduces the productivity at fish farms through either low feed efficiency or growth reduction of the fish. In addition to such an industrial problem, it was recently shown that lice from salmon farms can have an adverse impact on wild migratory salmonids by increasing the abundance of this parasite in bays and estuaries adjacent to the farms [1].

Different methods have been used in the fight against the sea lice infestation. In-feed treatments and usage of skirts (sheets hung around the salmon cages to prevent sea lice from entering) are very expensive methods. Skirts have low impact on the salmon welfare and the environment but reduce oxygen flow, which may cause a detrimental effect on fish respiratory functions [18].

Other methods such as cleaner fish, fresh water, physical removal measures, and veterinary medicines (sea lice have built up resistance to most of the chemicals that are used in medicines [19]) have environmental, health, and welfare impacts [19]. Less cost-effective methods include the use of hydrogen peroxide baths that, in addition, have effects on fish welfare and, consequently, on environmental and human health. From this perspective, the complexity of sea lice control requires a global holistic approach [18].

In this context, sound exposure methods can constitute an effective, innovative, and promising technology to address sea lice infestation. Our results showed the first ultrastructural images that characterize pathological changes in copepodids, chalimus, adult and pre-adults *L. salmonis* sensory first antenna setae after sound exposure. Essentially, the lesions were partial or complete fusions of the setae irregular branching tips of the first antenna. Fusion of fine sensory structures is typically the result of mechanical constraints due loud sound vibrations. Fusion of stereocilia has been shown to occur in statocysts sensory epithelium and lateral line systems of cephalopods [17,20] and in statocyst of cnidarians [14] after underwater noise exposure. Moreover, stereocilia fusion on auditory hair cells is a morphological characteristic of acoustic trauma in terrestrial animals [21,22]. Such pathological changes that directly affect the main *L. salmonis* sensory organ could make difficult finding of a host for a copepodid [8,9]. Additionally, exposed sea lice showed lesions on some distal pinnate setae on the caudal ramus and ventral arms. These abnormalities could provoke difficulties for the sea lice to move around the fish, which could also contribute to the decrease in the number of attachments to the salmons.

Moreover, to the best of our knowledge, this study shows the first published ultrastructural images of sea lice inner tissues affected by sound. The exposure affected the central nervous system of all analysed stages, likely altering their normal behaviour and challenging their survival as has been shown in other invertebrates [10,14]. In the copepodids and chalimus stages the A/B cells, which are responsible for the secretion of the precursor of frontal filament [7], were affected, thus probably challenging a correct anchoring to the fish. Similar lesions were shown on the tissues located in the same regions in both adults and pre-adults. In all of the stages, those lesions appear to be produced by autophagic and apoptotic processes [23–25].

Typical features of autophagic processes include the presence of numerous lysosomes and double-membrane-bounded vacuoles, "myelin-like formations" resulting from cell membrane destruction, large aggregates of dark material, and massive accumulation of ribosomes in the cell cytoplasm. Interestingly, in our exposed tissues we could follow the normal evolution sequence from primary to mature secondary lysosome with decreasing activity, which posteriorly released its content to an adjacent autophagosome [26,27]. The presence of a large amount of secondary lysosomes and residual bodies in the exposed animals is a clear sign of the extreme functioning of the cytological mechanisms caused by the stress situation originated after sound exposure. Moreover, the frequent presence of large areas of empty cytoplasm was the hallmark of advanced stages of cell degeneration through autophagy. Beside autophagy, pathological features such as deformed cell nuclei,

chromatin compaction into the nuclei, and cytoplasm condensation strongly suggest the occurrence of apoptotic processes.

The mechanisms by which sound induced massive autophagy and apoptosis in the present specimens, have yet to be precisely determined. One possible hypothesis is that acoustic exposure primarily induced an oxidative stress that is known to regulate the expression of both autophagy and apoptosis [28]. In support of the oxidative stress hypothesis, the accumulation of dark inclusions around the eye could correspond to mitochondrial autophagic profiles. Mitochondria in fact play a key role in oxidative stress [29–31], and autophagy-damaged mitochondria has been described as the effect of sound exposure in the optic nerve [22]. Another possibility is that part of the dark inclusions was due to hyperpigmentation. Hyperpigmentation actually may occur as a consequence of an oxidative stress following acoustic trauma in several tissues, including the eyes [32].

Altogether, the present study indicates that the central nervous system in all stages and the A/B cells (responsible for the secretion of the precursor of frontal filament) [7] in copepodids and chalimus stages were affected by sound exposure. These encouraging findings therefore indicate that sound exposure can lead to severe consequences on the capacity of the sea lice to infest its host. The present results were completed by an exhaustive health status analysis of the exposed salmons [33] that showed that the use of these frequency combinations did not affect the fish. In this assessment through gross pathology and histopathological analysis, salmons didn't show any lesion that could be related to sound exposure. In addition, the analysis of the otolith's organs did not show any effects on the auditory organs of the fish. Although some consequences of the sound-induced lesions found in lice remain to be further studied, this method constitutes a promising approach to address lice plagues while also reducing the need for chemical treatments of the fish.

5. Patents

André M., Solé M., Van der Schaar, De Vreese S (International Patent WO 2018/167003 A1). 20-09-2018. A method for inducing lethal lesions in sensory organs of undesirable aquatic organisms by use of sound. Licensed to SEASEL SOLUTIONS AS [NO/NO]; P.O. BOX 93 N-6282 BRATTVÅG (NO).

André M., Solé M., Van der Schaar (Norwegian patent WO/2020/048945). 03-09-2019. System and method for reducing sea lice exposure in marine fish farming. Licensed to SEASEL SOLUTIONS AS [NO/NO]; P.O. BOX 93 N-6282 BRATTVÅG (NO).

Conflicts of Interest: The authors declare no conflict of interest.

References

1. Whelan, K.A. Review of the Impacts of the Salmon Louse, *Lepeophtheirus salmonis* (*Krøyer, 1837*) on Wild Salmonids. Atl. Salmon Trust **2010**. Available online: https://atlanticsalmontrust.org/wp-content/uploads/2016/12/ast-sea-lice-impacts-review1.pdf (accessed on 12 May 2021).
2. Revie, C.; Dill, L.; Finstad, B.; Todd, C. *Sea Lice Working Group Report*; NINA Special Report 39; World Wildlife Fund: Norway. Available online: http://www.nina.no/archive/nina/pppbasepdf/temahefte/039.pdf (accessed on 12 May 2021).
3. Thorstad, E.; Todd, C.; Uglem, I.; Alamaru, A.; Bronstein, O. Effects of salmon lice *Lepeophtheirus salmonis* on wild sea trout, Salmo trutta—A literature review. *Aquac. Environ. Interact.* **2015**, *7*, 91–113. [CrossRef]
4. Wagner, G.; Fast, M.; Johnson, S. Physiology and immunology of *Lepeophtheirus salmonis* infections of salmonids. *Rev. Cell.* **2008**, *24*, 176–183. [CrossRef]
5. Mordue, A.; Birkett, M. A review of host finding behaviour in the parasitic sea louse, *Lepeophtheirus salmonis (Caligidae: Copepoda)*. *J. Fish Dis.* **2009**, *32*, 3–13. [CrossRef] [PubMed]
6. Strickler, J.; Bal, A. Setae of the first of the copepod *Cyclops scutifer* (Sars): Their structure and importance. *Proc. Natl. Acad. Sci. USA* **1973**, *70*, 2656–2659. [CrossRef] [PubMed]
7. Gonzalez-Alanis, P.; Wright, G.M.; Johnson, S.C.; Burka, J.F. Frontal filament morphogenesis in the salmon louse *Lepeophtheirus salmonis*. *J. Parasitol.* **2001**, *87*, 561–574. [CrossRef]
8. Heuch, P.A.; Karlsen, E. Detection of infrasonic water oscillations by copepodids of *Lepeophtheirus salmonis* (Copepoda 10.1093/plankt/19.6.735, Caligida). *J. Plankton Res.* **1997**, *19*, 735–747. [CrossRef]
9. Heuch, P.A.; Doall, M.H.; Yen, J. Water flow around a fish mimic attracts a parasitic and deters a planktonic copepod. *J. Plankton Res.* **2007**, *29*, i3–i16. [CrossRef]
10. Solé, M.; Sigray, P.; Lenoir, M.; van der Schaar, M.; Lalander, E.; André, M. Offshore exposure experiments on cuttlefish indicate received sound pressure and particle motion levels associated with acoustic trauma. *Sci. Rep.* **2017**, *7*, 45899. [CrossRef]
11. Solé, M.; Fortuño, J.-M.; van der Schaar, M.; André, M. An acoustic treatment to mitigate the effects of the apple snail on agriculture and natural ecosystems. *J. Mar. Sci. Eng.* **2021**, *9*.
12. Day, R.D.; McCauley, R.D.; Fitzgibbon, Q.P.; Hartmann, K.; Semmens, J.M. Seismic air guns damage rock lobster mechanosensory organs and impair righting reflex. *Proc. R. Soc. B Biol. Sci.* **2019**, *286*, 20191424. [CrossRef] [PubMed]
13. Day, R.D.; McCauley, R.D.; Fitzgibbon, Q.P.; Hartmann, K.; Semmens, J.M. Exposure to seismic air gun signals causes physiological harm and alters behavior in the scallop Pecten fumatus. *Proc. Natl. Acad. Sci. USA* **2017**, *114*, E8537–E8546. [CrossRef]
14. Solé, M.; Lenoir, M.; Fontuño, J.M.; Durfort, M.; van der Schaar, M.; André, M. Evidence of Cnidarians sensitivity to sound after exposure to low frequency noise underwater sources. *Sci. Rep.* **2016**, *6*, 37979. [CrossRef] [PubMed]
15. Fuchs, H.L.; Christman, A.J.; Gerbi, G.P.; Hunter, E.J.; Diez, F.J. Directional flow sensing by passively stable larvae. *J. Exp. Biol.* **2015**, *218*, 2782–2792. [CrossRef]
16. Johnson, S.; Albright, L. The developmental stages of *Lepeophtheirus salmonis* (Kroyer, 1837) (Copepoda:Caligidae). *Can. J. Zool.* **1991**, *69*, 929–950. [CrossRef]
17. Solé, M.; Lenoir, M.; Durfort, M.; López-Bejar, M.; Lombarte, A.; van der Schaar, M.; André, M. Does exposure to noise from human activities compromise sensory information from cephalopod statocysts? *Deep. Res. Part II Top. Stud. Oceanogr.* **2013**, *95*, 160–181. [CrossRef]
18. Barrett, L.T.; Oppedal, F.; Robinson, N.; Dempster, T. Prevention not cure: A review of methods to avoid sea lice infestations in salmon aquaculture. *Rev. Aquac.* **2020**, *12*, 2527–2543. [CrossRef]
19. Hannisdal, R.; Nøstbakken, O.J.; Hove, H.; Madsen, L.; Horsberg, T.E.; Lunestad, B.T. Anti-sea lice agents in Norwegian aquaculture; surveillance, treatment trends and possible implications for food safety. *Aquaculture* **2020**, *521*, 735044. [CrossRef]
20. Solé, M.; Lenoir, M.; Fortuño, J.-M.; van der Schaar, M.; André, M. A critical period of susceptibility to sound in the sensory cells of cephalopod hatchlings. *Biol. Open* **2018**, *7*, bio033860. [CrossRef]
21. Engström, B. Stereocilia of sensory cells in normal and hearing impaired ears. A morphological, physiological and behavioural study. *Scand. Audiol. Suppl.* **1983**, *19*, 1–34. [PubMed]
22. Liberman, M. Chronic ultrastructural changes in acoustic trauma: Serial-section reconstruction of stereocilia and cuticular plates. *Hear. Res.* **1987**, *26*, 65–88. [CrossRef]
23. D'Arcy, M.S. Cell death: A review of the major forms of apoptosis, necrosis and autophagy. *Cell Biol. Int.* **2019**, *43*, 582–592. [CrossRef] [PubMed]
24. Glick, D.; Barth, S.; MacLeod, K.F. Autophagy: Cellular and molecular mechanisms. *J. Pathol.* **2010**, *221*, 3–12. [CrossRef]
25. Elmore, S. Apoptosis: A review of programmed cell death. T.P. 2007 J.-516. Apoptosis: A review of programmed cell death. *Toxicol. Pathol.* **2007**, *35*, 495–516. [CrossRef]
26. Liberge, M.; Gros, O.; Frenkiel, L. Lysosomes and sulfide-oxidizing bodies in the bacteriocytes of Lucina pectinata, a cytochemical and microanalysis approach. *Mar. Biol.* **2001**, *139*, 401–409. [CrossRef]
27. Trivedi, P.C.; Bartlett, J.J.; Pulinilkunnil, T. Lysosomal Biology and Function: Modern View of Cellular Debris Bin. *Cells* **2020**, *9*, 1131. [CrossRef] [PubMed]

28. Kaminskyy, V.O.; Zhivotovsky, B. Free radicals in cross talk between autophagy and apoptosis. *Antioxid. Redox Signal.* **2014**, *21*, 86–102. [CrossRef] [PubMed]

29. Peoples, J.N.; Saraf, A.; Ghazal, N.; Pham, T.T.; Kwong, J.Q. Mitochondrial dysfunction and oxidative stress in heart disease. *Exp. Mol. Med.* **2019**, *51*, 1–13. [CrossRef]

30. Lejri, I.; Agapouda, A.; Grimm, A.; Eckert, A. Mitochondria- and Oxidative Stress-Targeting Substances in Cognitive Decline-Related Disorders: From Molecular Mechanisms to Clinical Evidence. *Oxid. Med. Cell Longev.* **2019**, *2019*, 1–26. [CrossRef]

31. Subramaniam, S.R.C.M. Mitochondrial dysfunction and oxidative stress in Parkinson's disease. *Prog. Neurobiol.* **2013**, *106–107*, 17–32. [CrossRef]

32. Taubitz, T.; Tschulakow, A.V.; Tikhonovich, M.; Illing, B.; Fang, Y.; Biesemeier, A.; Julien-Schraermeyer, S.; Schraermeyer, U. Ultrastructural alterations in the retinal pigment epithelium and photoreceptors of a Stargardt patient and three Stargardt mouse models: Indication for the central role of RPE melanin in oxidative stress. *PeerJ* **2018**, *2018*, e5215. [CrossRef]

33. Solé, M.; Constenla, M.; Padrós, F.; Lombarte, A.; Fortuño, J.M.; André, M. Farmed salmons show no pathological alterations when exposed to acoustic sea lice infestation treatment. *J. Mar. Sci. Eng.* **2021**, *9*.